ISBN: 978-3-95450-247-9 ISSN: 2673-5490 doi: 10.18429/JACoW-IPAC2024-TUPG28

BESSY III OVERVIEW AND ITS BENDING SOURCES*

P. Goslawski†, M. Abo-Bakr, M. Arlandoo, K. Holldack,
A. Jankowiak, B. Kuske, J. Viefhaus, J. Völker
Helmholtz-Zentrum Berlin, BESSY, Berlin, Germany

Abstract

The BESSY III project evolves from a pre-CDR phase into the CDR phase. And for lattice design, it means, that one of the different Higher-Order-Achromat MBA lattice candidates has to be chosen as the baseline lattice for the iterations with the construction department. Therefore it is essential that the At BESSY III, it is requested, that the bends be used as bending sources in different regimes, the soft-X-ray (<2 keV), in the tender (2-10 keV), and hard X-rays (>10 keV). In this contribution, we will give an overview of the BESSY III project and its bending sources and discuss briefly the baseline lattice.

INTRODUCTION

HZB is preparing for its future light source with two main projects [1]: the BESSY II+ project and BESSY III. BESSY II+ is a refurbishment and modernization project of the exiting 1.7 GeV BESSY II facility with the main focus on operando capabilities in the experimental hall, to enable state-of-the-art operation for the next decade. It will act as a bridge towards BESSY III helping to shape the science case and driving technology developments [2]. The BESSY III project aims to establish a greenfield 4th generation light source based on a 6-MBA (multi-bend-achromat) lattice. A first sketch of the facility was recently published in a "Pre-Conceptual Design Report" [3].

THE BASELINE LATTICE

The lattice design process is extensively described and summarized in [4] and references therein. To deliver a robust design with good control of non-linear beam dynamics, we chose the Higher-Order Achromat (HOA) approach [5], fixing the phase advance between the distributed and repetitive two chromatic sextupole families within the MBA structure.

Due to the necessarily low dispersion and the strong focusing of MBA lattices, their strong sextupoles lead to demanding non-linear behavior. Since the non-linearities in the transverse plane limit the performance of many[1] MBA lattices, we focused right from the beginning of the lattice design process on relaxing the transverse non-linear beam dynamics, despite providing the required emittance 100 pm rad. Therefore we followed a systematic and deterministic lattice design approach [6]. We studied in detail the various possibilities to set up the different basic building blocks of an MBA lattice, which are the inner MBA-unit-cell (UC), the dispersion suppression cell (DSC), and the dispersion free matching cell (MC) to reduce the sextupole power needed for the correction of the transverse natural chromaticity and provide the necessary phase matching for cancellation of the lower order resonance driving terms. For the MBA-UC, which consists of the main bend, two focusing, and two chromaticity correcting components in the x-plane and y-plane respectively, we could show that utilizing a setup build-up on a **s**eparated **f**unction (**sf**) bend reduces the sextupole power by factor 2, resulting in a factor ~2 better momentum acceptance compared to a **c**ombined **f**unction (**cf**) bend solution. Comparing lattices with only two sextupole families for correcting the horizontal and vertical natural chromaticity [4] the momentum acceptance is limited to 2 % for the cf lattices and extends to 3.8 % for the best sf lattice. By splitting up the sextupoles families and introducing chromatic octupoles, it can be improved to ~3 % for cf and ~5 % for sf[2].

To circumvent issues with non-linearities in the longitudinal plane & collective effects described during the SLS2.0 design process [7,8] for very small or even negative momentum compaction factor, α_0, the design value for BESSY III was set to $\alpha_0 > 1.0 \times 10^{-4}$ from the beginning. However, the two solutions (sf, cf) show different longitudinal behavior, which will be described in the following.

Non-Linearities in the Longitudinal Plane

Figure 1 (left) shows the comparison of the development of the momentum acceptance in the longitudinal plane, i.e., the rf bucket height for the cf and sf lattice, when increasing the rf voltage. Whereas the cf lattice shows saturation at 2.3 MV and ~8 % momentum acceptance, the sf lattice is limited much earlier in voltage at 0.9 MV and ~3.7 % momentum acceptance.

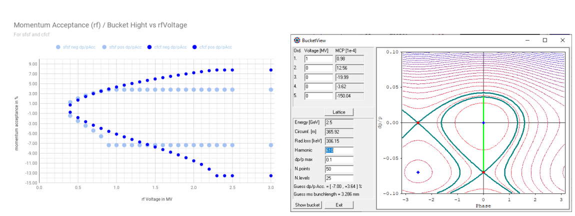

(a) (b)

Figure 1: RF momentum acceptance in the longitudinal plane.

The reason for the limitation are the non-linear higher order contributions to the momentum compaction factor and dispersion. These non-linearities start to dominate the

* Work supported by German Bundesministerium für Bildung und Forschung, Land Berlin, and grants of Helmholtz Association
† paul.goslawski@helmholtz-berlin.de
1 "maybe all"
2 In this stage of the design process the numbers belong to bare lattices without errors.

© Content from this work may be used under the terms of the CC BY 4.0 licence (© 2024). Any distribution of this work must maintain attribution to the author(s), title of the work, publisher, and DOI.

ISBN: 978-3-95450-247-9 ISSN: 2673-5490 doi: 10.18429/JACoW-IPAC2024-TUPG28

longitudinal phase space, i.e., the oscillation in phase and momentum deviation $\delta = \Delta p/p_0$, see Fig. 1 (right) and might become a problem for "quasi-isochronous storage rings" [9]. That means, that higher orders of the momentum compaction factor

$$\Delta L/L_0 = \alpha(\delta)\,\delta = \alpha_0\,\delta + \alpha_1\,\delta^2 + \ldots \tag{1}$$

$$\alpha_0 = \frac{1}{L_0}\oint \frac{D}{\rho} ds \tag{2}$$

$$\alpha_1 = \frac{1}{L_0}\oint \frac{D'^2}{2} + \frac{D_1}{\rho} ds \tag{3}$$

and of the dispersion

$$x = x_\beta + D\,\delta + D_1\,\delta^2 + \ldots \tag{4}$$

will define the dynamics. The ratio of $\frac{\alpha_0}{\alpha_1}$ defines the balance between the on-momentum unstable fixed point, which determines the well-known fish-like rf bucket and the off-momentum unstable fixed point which, if dominating, limits the momentum acceptance independent of the rf voltage. The ratio is $\frac{\alpha_0}{\alpha_1} = \frac{1.1}{5.5}$ for the cf-lattice and $\frac{\alpha_0}{\alpha_1} = \frac{1.0}{12.1}$ for the sf-lattice. Since all lattice candidates have been constructed in a way to achieve a momentum compaction factor $\alpha_0 \geq 1.0 \times 10^{-4}$, the limit is given by α_1.

Inspecting Eq. (3), there must be a difference between the two lattices (cf & sf) in the derivative of the dispersion D' and/or the 2[nd] order dispersion D_1. Both quantities are plotted for the two lattices in Fig. 2 (left). The right plot shows their individual contribution to the integral $\frac{D'^2}{2}$ (red) and $\frac{D_1}{\rho}$ (blue). Clearly, the additional vertically focusing

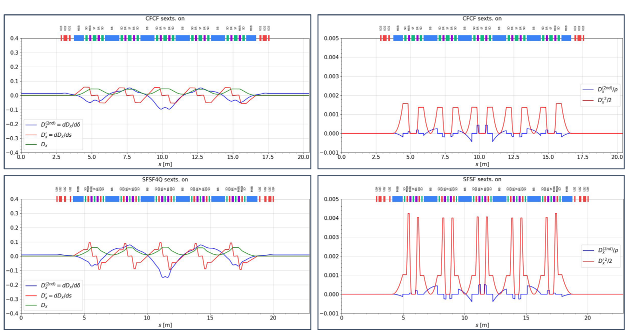

Figure 2: Origins for the high α_1 - the non-linearities in the longitudinal plane.

quadrupole in the sf lattices applies an additional kick to the dispersion, which is best seen in its derivative (red). Since the dispersion derivative contributes quadratically to the integral, it is the driving factor for the larger α_1 and the momentum acceptance limit in the longitudinal plane for the sf lattice. The contribution of the 2[nd] order dispersion D_1 is negligible.

Unfortunately, in terms of momentum acceptance for both kinds of lattice candidates, it is a very mal-adjusted situation:

- **The cfcf-lattice** provides 2-3% momentum acceptance in the transverse plane and ~8 % in the longitudinal plane.
- **The sfsf-lattice** has 4-5% momentum acceptance in the transverse plane and only ~3.7 % in the longitudinal plane.

Especially the situation of the sf-lattice is unsatisfactory. The additional vertically focusing quadrupole, which increases the decoupling of the β-functions at the positions of the chromatic sextupoles and improves the transverse momentum acceptance, kicks the despersion, which limits the momentum acceptance in the longitudinal plane. The individual basic blocks of the lattice (UC, DSC, MC) have been investigated once more to increase α_0 and to reduce α_1 and find a better matching of momentum acceptances in the transverse and longitudinal plane. The most effective countermeasures have been the reduction of the main bend angle and balancing more bending in the DSC bend and the increase of main bend length. Both reduced the emittance and allow to reduce the RB angle. In addition the RB was omitted or reduced in the DSC. This allowed to reduce the non-linearities in the longitudinal plane to $\frac{\alpha_0}{\alpha_1} = \frac{1.3}{9.4}$, improving the longitudinal momentum acceptance to ~6 %.

With a first non-linear optimization using OPA[3], i.e., by splitting up the two sextupole families into individual magnets and the introduction of one chromatic "mainly" horizontally-acting octupole in the DSC the transverse momentum acceptance could be improved to nearly 5 %, which suits very well to the longitudinal one. Currently, we are working to develop a well-defined recipe to optimize the non-linear knobs and beam dynamics [11]. The BESSY III baseline lattice with its most important parameters is shown in Fig. 3.

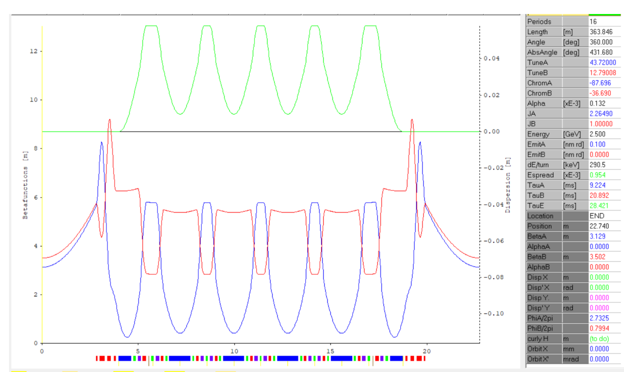

Figure 3: The BESSY III baseline lattice.

Bending Magnets as Radiation Sources

The flux density and the brilliance of the bending sources at BESSY II and the intended bending sources at BESSY III are shown in Fig. 4. BESSY II currently provides two different types of bending sources: Homogeneous bends based on iron yoke electromagnets at 1.3 T@1.7 GeV, which provide a critical photon energy of 2.5 keV (blue) and superconducting wavelength shifters with 7 T@1.7 GeV, providing a critical photon energy of 13 keV (orange).

[3] see `https://ados.web.psi.ch/opa/index.html`

Content from this work may be used under the terms of the CC BY 4.0 licence (© 2024). Any distribution of this work must maintain attribution to the author(s), title of the work, publisher, and DOI.

ISBN: 978-3-95450-247-9 ISSN: 2673-5490 doi: 10.18429/JACoW-IPAC2024-TUPG28

© Content from this work may be used under the terms of the CC BY 4.0 licence (© 2024). Any distribution of this work must maintain attribution to the author(s), title of the work, publisher, and DOI.

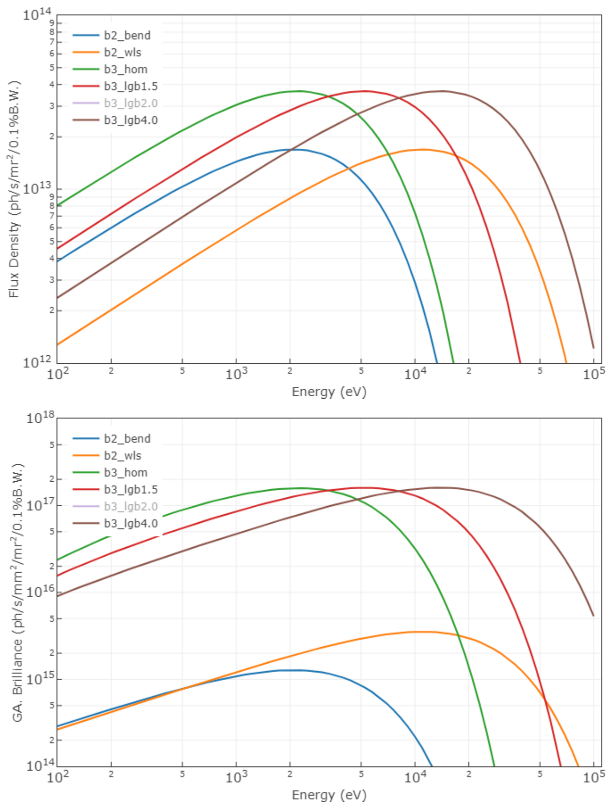

Figure 4: Flux and brilliance of different bending sources at BESSY II (blue and orange) and of bending sources discussed for BESSY III (green, red, and brown).

For BESSY III users request also bending beamlines with different spectral ranges, from EUV to soft X-rays (0.01 keV to 2 keV), from soft to tender X-rays (2 keV to 10 keV) and hard X-rays (≥10 keV).

For geometric reasons, radiation can be best extracted from three inner dipole magnets (#2, #3, #4) of the arc of the BESSY III 6-MBA sector, shown in Fig. 5 (top). It is foreseen to provide at least one bending beamline per arc, two might also be possible.

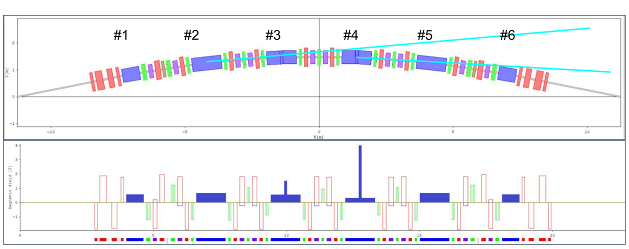

Figure 5: (top) The magnetic arrangement of a BESSY III sector (bends - blue, quadrupoles - red, reverse bends (shifted quadrupoles) - purple, sextupoles - green). (bottom) The magnetic peak field for the different magnets.

The standard homogeneous bend at BESSY III based on permanent magnets technology with 0.64 T@2.5 GeV does nicely match PTB's needs for metrology applications, providing a critical photon energy of 2.6 keV (green) and delivers nearly the same spectral range as the bending magnet at BESSY II, but increases the flux density by a factor 2 and the brilliance by 100, as shown in Fig. 4. It is under discussion if the request for higher photon energies can be covered by longitudinal gradient bends (LGB). As a first guess, the homogeneous bend was separated into three areas supplying a higher field at the center and reduced fields at the beginning and end, see Fig. 5 (bottom). Initial studies showed no severe impact on the beam dynamics when modifying the main bend as long as the phase advances over the MBA-UC and the matching conditions for the optical functions are maintained. Without changing the vacuum pipe diameter a field of up to 1.5 T could be possible using permanent magnet solutions, which would provide a critical photon energy of 6.2 keV (red). A superconducting solution with 4 T would push the critical energy up to 16.3 keV, but this solution needs more technical R&D and would increase the project risks. So far, our investigations show no notable emittance-reducing impact of the LGB. As the phase advance is kept constant and the optical functions are not adapted to the higher field, no emittance-reducing effect is expected. Further studies should investigate the impact of adjusted optical functions on the overall performance with LGBs. So far, it is foreseen to use the LGBs as adapted bending sources.

CONCLUSION & OUTLOOK

In a careful process, focusing on suppressing non-linear beam dynamics contributions, a BESSY III baseline lattice was developed based on a 6-MBA HOA with separate function dipoles. Limitations of the longitudinal momentum acceptance were analyzed and could be mitigated without corrupting other design criteria. Plans for supplying different wavelengths from the bending magnets were introduced. For moderate field increase and/or a limited number of higher field bending magnets, no relevant deterioration of the dynamic was observed. As the next steps, we are looking forward to pushing the BESSY III lattice toward the TDR phase (technical adaption, injection straight, robustness against errors, collective effects, ...).

ACKNOWLEDGEMENTS

The authors would like to thank A. Streun for the fruitful discussion.

REFERENCES

[1] A. Vollmer *et al.*, "Materials Discovery at BESSY", *Synchrotron Radiation News*, vol. 37, no. 1, pp. 12–17, Feb. 2024. doi:10.1080/08940886.2024.2312051

[2] P. Goslawski *et al.*, "BESSY III - status and overview", in *Proc. IPAC'23*, Venice, Italy, May 2023, pp. 457–460. doi:10.18429/JACoW-IPAC2023-MOPA174

[3] P. Goslawski *et al.*, "BESSY III - The Materials Discovery Facility", Helmholtz-Zentrum Berlin, Germany, Pre-Conceptual Design Report, 2022. doi:10.5442/r0004

ISBN: 978-3-95450-247-9 ISSN: 2673-5490 doi: 10.18429/JACoW-IPAC2024-TUPG28

[4] P. Goslawski *et al.*, “Update on the lattice design process of BESSY III: towards a baseline lattice”, in *Proc. IPAC’23*, Venice, Italy, May 2023, pp. 3196–3199. doi:10.18429/JACoW-IPAC2023-WEPL036

[5] J. Bengtsson, “The Sextupole Scheme for the Swiss Light Source (SLS): An analytic appraoch”, Paul Scherrer Institut (PSI), Villigen, Switzerland, Rep. SLS Note 9/97, 7 Mar. 1997. https://ados.web.psi.ch/slsnotes/sls0997.pdf

[6] B. Kuske and P. Goslawski, “Deterministic Approach to MBA Lattice Design”, presented at iFAST – 9th Low Emittance Workshop, CERN, Switzerland, 2024, https://indico.cern.ch/event/1326603/contributions/5773933/

[7] A. Streun *et al.*, “SLS-2 – the upgrade of the Swiss Light Source”, *Synchrotron Radiation News*, pp. 631-641, 2018. doi:10.1107/S1600577518002722

[8] M. M. Dehler, M. Aiba, A. Citterio, and L. Stingelin, “Overview of Collective Effects in SLS 2.0”, in *Proc. IPAC’19*, Melbourne, Australia, May 2019, pp. 1658–1661. doi:10.18429/JACoW-IPAC2019-TUPGW107

[9] D. Robin *et al.*, “Quasi-isochronous storage rings”, *Phys. Rev. E*, vol. 48, pp. 2149-2156. doi:10.1103/PhysRevE.48.2149

[10] A. Streun, “OPA-Lattice Design Code”, https://ados.web.psi.ch/opa/

[11] B. Kuske, A. Santamaria Garcia, and M. Arlandoo, “Comparison of multi-objective Bayesian optimization and the reduction of resonance driving terms in the optimization of the dynamic aperture of the BESSY III MBA lattice”, presented at the IPAC’24, Nashville, TN, USA, May 2024, paper MOPS14, this conference.

© Content from this work may be used under the terms of the CC BY 4.0 licence (© 2024). Any distribution of this work must maintain attribution to the author(s), title of the work, publisher, and DOI.